J. Phycol. **40,** 557–567 (2004)

DOI: 10.1111/j.1529-8817.2004.03184.x

INDUCTION OF PHOTORESPIRATION BY LIGHT IN THE CENTRIC DIATOM *THALASSIOSIRA WEISSFLOGII* (BACILLARIOPHYCEAE): MOLECULAR CHARACTERIZATION AND PHYSIOLOGICAL CONSEQUENCES[1]

Micaela Schnitzler Parker, E. Virginia Armbrust[2]

Marine Molecular Biotechnology Laboratory, School of Oceanography, University of Washington, Seattle, Washington 98195, USA

Jonah Piovia-Scott and Richard G. Keil

School of Oceanography, University of Washington, Seattle, Washington 98195, USA

Glycine decarboxylase (GDC) is a multi-subunit enzyme that plays a key role in the photorespiratory pathway. A cDNA (*GDCT*) with a deduced amino acid sequence sharing up to 64% homology and 50% identity with the T-protein subunit of GDC from land plants was identified from the centric diatom *Thalassiosira weissflogii* (Grun.) Fryxell et Hasle. The effect of light on transcript abundance was determined using competitive RT-PCR. *GDCT* mRNA per cell decreased during prolonged dark incubations and was higher in cells grown at higher light intensities, independent of growth rate. Cells acclimated to a 12:12-h light:dark cycle maintained the same amount of *GDCT* transcripts before and after the dark phase, but rapidly increased transcript levels in the light with a peak "mid-day." Rapid increases in *GDCT* message abundance also occurred in response to an increase in irradiance. Transcript abundance of *twca1*, the gene for carbonic anhydrase, was also measured and displayed a slower and much less pronounced response to changes in light intensity. An HPLC-based method was used to measure the concentration of the photorespiratory-specific compound glycolate in the culture media. Only cultures shifted from low subsaturating irradiances to the highest light intensity released significant amounts of glycolate. Our results suggest that quantifying *GDCT* mRNA in conjunction with measurements of glycolate will allow us to monitor both the initiation of photorespiration and its physiological consequences in the marine environment.

Key index words: **diatom; glycine decarboxylase; glycolate; photorespiration; *Thalassiosira weissflogii*; transcript**

Abbreviations: **CCM, carbon-concentrating mechanism; DOC, dissolved organic carbon; GDC, glycine decarboxylase; *GDCT*, cDNA for GDC T-protein; RACE, rapid amplification of cDNA ends**

Photorespiration occurs when O_2 outcompetes CO_2 for binding with the carbon-fixation enzyme RUBISCO. Fixation of O_2 rather than CO_2 results in the formation of a two-carbon molecule, 2-P-glycolate, that cannot enter the Calvin cycle. Instead, 2-P-glycolate is metabolized in the photorespiratory pathway, producing a succession of organic carbon and nitrogen compounds including glycolate, glycine, and serine. Ultimately, 3-P-glycerate is generated and enters the Calvin cycle. However, one of every four carbons that enters the photorespiratory pathway is used to produce CO_2 (Oliver 1998), and the conversion of glycine to serine results in the formation of NH_3 (Keys et al. 1978). In marine algae, high light and high concentrations of O_2 are known to enhance photorespiration (Beardall 1989) and promote leakage of organics such as the photorespiratory-specific compound glycolate (Hellebust 1965, Al-Hasan and Coughlan 1976, Fogg 1983). Thus, photorespiration may play a key role in mediating the release of fixed carbon and nitrogen from cells under conditions of high light or high O_2.

In the marine environment, phytoplankton often experience both high light and high O_2 concentrations concurrently during a bloom. Rapid increases in growth and cell division that define a bloom are dependent on the availability of light, and the resulting increase in photosynthesis can dramatically saturate the surrounding seawater with oxygen (Duxbury et al. 2000). Blooms are often associated with carbon and nitrogen fluxes out of the mixed layer because of aggregation and sinking of cells (Scharek et al. 1999) or packaging of cells into fecal pellets (Buck and Newton 1995). However, evidence suggests that as much as 10%–30% of the carbon fixed by phytoplankton is released as dissolved organic matter (Baines and Pace 1991, Malinsky-Rushansky and Legrand 1996, Nagata 2000), often in response to a physiological stress such as exposure to high light (Verity 1981, Chrost and Faust 1983, Zlotnik and Dubinsky 1989). The contribution of photorespiration to the release of dissolved organic carbon (DOC) from phytoplankton cells has been estimated under laboratory conditions to be about 5%–40% (Al-Hasan and Coughlan 1976, Fogg 1983, Leboulanger et al. 1998). However, it is inherently difficult to assess the contribution of photore-

[1]Received 3 October 2003. Accepted 10 March 2004.
[2]Author for correspondence: e-mail armbrust@ocean.washington.edu.

spiration to DOC release in the field because of the rapid turnover of its products.

The primary means for detecting photorespiration in the field is the measurement of the photorespiratory-specific compound, glycolate. Leboulanger et al. (1997) found high concentrations of glycolate in seawater from oligotrophic to eutrophic sites, suggesting photorespiration may be ubiquitous in the pelagic environment. Concentrations of glycolate were also found to increase during the day and to decrease at night. This lead to the hypothesis that during the day production by phytoplankton likely outpaced uptake by heterotrophs, whereas at night net heterotrophic uptake occurred. Laboratory studies have shown that glycolate is metabolized by many species of marine bacteria (Wright and Shah 1975, Pant and Fogg 1976, W. W. Y. Lau, personal communication). Therefore, the concentration of glycolate in seawater is likely a factor of both production by phytoplankton and uptake by bacteria, suggesting that bulk glycolate concentrations may underestimate photorespiration in field samples.

In this study we focused on finding an internal molecular marker with the potential for monitoring photorespiration in diatoms. Diatoms are frequently dominant components of phytoplankton blooms (Nelson et al. 1995) and are often associated with carbon and nitrogen export (Longhurst and Harrison 1989). The marker we chose is the gene for a central enzyme of the photorespiratory pathway, glycine decarboxylase (GDC). Together with serine hydroxymethyltransferase, GDC catalyzes the conversion of two glycine molecules into one serine with the consequent release of CO_2 and NH_3 in the mitochondria. In heterotrophs, GDC is used in catabolism of both glycine and serine (Kikuchi and Hiraga 1982). In autotrophs, GDC may be used in biosynthesis of amino acids, but the primary use of this enzyme is in photorespiration (Oliver et al. 1990, Mouillon et al. 1999). An increase in both glycine and serine due to the metabolism of glycolate during photorespiration has been observed in several marine algae (Burris 1977, Leboulanger et al. 1998). GDC is an enzyme composed of four subunits, denoted L-, P-, H-, and T-protein. Transcription of the genes for the H-, T-, and P-proteins are light dependent in land plants consistent with photorespiration as a light-dependent pathway (Turner et al. 1993, Vauclare et al. 1998). Here, we report the full-length sequence of a cDNA (*GDCT*) from the centric diatom *Thalassiosira weissflogii* that we hypothesize encodes the T-protein of GDC. We further demonstrate the dependence of *GDCT* transcript abundance on light. In addition, we quantify the cellular release of glycolate under experimental conditions establishing a link between *GDCT* transcript abundance and photorespiration.

MATERIALS AND METHODS

Culture conditions. Axenic cultures of *T. weissflogii* Grun. (Provasoli-Guillard National Center for Culture of Marine Phytoplankton, CCMP1336 clone Actin isolated from Long Island Sound, NY, USA) were maintained at 20° C in sterile f/2 medium (Guillard 1975) in exponential growth using semicontinuous batch cultures (Brand et al. 1981). Cultures were swirled daily and acclimated to four continuous light intensities (cool-white fluorescent bulbs): 15, 50, 150, and 400 μmol photons $\cdot m^{-2} \cdot s^{-1}$. Based on previous work with *T. weissflogii* by Armbrust et al. (1990), the four light intensities included one at growth saturation (150 μmol photons $\cdot m^{-2} \cdot s^{-1}$), one well above growth saturation (400 μmol photons $\cdot m^{-2} \cdot s^{-1}$), and two subsaturating irradiances (15 and 50 μmol photons $\cdot m^{-2} \cdot s^{-1}$). Additional cultures were maintained in exponential growth on a 12:12-h light:dark cycle of 100 μmol photons $\cdot m^{-2} \cdot s^{-1}$ at 20° C. *In vivo* chl *a* fluorescence was monitored daily with a 10-AU fluorometer (Turner Designs, Sunnyvale, CA, USA). Cultures acclimated to a light:dark cycle were measured just before the end of the dark period. When the slopes from three or more growth curves were no longer significantly different (F-test, Zar 1996), the culture was considered acclimated. Growth rates were determined from the change in fluorescence of three successive transfers after acclimation. For experiments, cells were grown in 500-mL or 1-L flasks in 250 mL or 500 mL of media, respectively. To minimize nutrient limitation effects, experiments were started when cultures were in early exponential growth (approximately 20,000 cells $\cdot mL^{-1}$) and terminated before late exponential growth (approximately 80,000 cells $\cdot mL^{-1}$).

Cloning and sequencing. Clones from a partial cDNA library (Armbrust 1999) were sequenced using plasmid DNA prepared with the Qiaprep Spin Miniprep kit (Qiagen Inc., Valencia, CA, USA) and cycle sequenced with M13 forward and reverse primers and a Thermo Sequenase II Dye Terminator Cycle Sequencing Kit (Amersham Biosciences Corp., Piscataway, NJ, USA). Sequences were analyzed using an ABI 373A automated sequencer (Applied Biosystems, Foster City, CA, USA). One partial cDNA was chosen for further sequencing because the predicted protein displayed high homology to the T-protein of glycine decarboxylase (GDCT). The full-length *GDCT* cDNA was generated using rapid amplification of cDNA ends (RACE). RACE PCR primers to adaptor sequence (AP1, BD Biosciences Clontech, Palo Alto, CA, USA) and gene-specific primers were used to amplify the 5′ and 3′ ends of the *GDCT* cDNA using Advantage cDNA polymerase mix (Clontech) in a 20-μL reaction containing 4 pmol of each primer and 0.4 mM dNTPs. The RACE profile began with an initial denaturation step of 94° C for 1 min followed by 5 cycles of 94° C for 30 s, 72° C for 4 min; 5 cycles of 94° C for 30 s, 70° C for 4 min; 25 cycles of 94° C for 20 s, 68° C for 4 min. Amplified fragments were ligated into the pCR2.1-TOPO vector and used to transform TOP10 *Escherichia coli* cells (TOPO TA cloning kit, Invitrogen Corp., Carlsbad, CA, USA). Plasmid minipreps of positive clones were generated and inserts cycle sequenced as described above. New gene-specific primers were developed and the process repeated until the initiator methionine sequence ATG (5′ end) and the poly(A) tail (3′ end) were identified. The GenBank accession number for the full-length *GDCT* cDNA is AY375364. Predicted amino acid sequences were aligned using ClustalW (Thompson et al. 1994) in BioEdit v. 5.0.9 (Hall 1999).

Sampling and RNA extraction. For each light induction experiment, cells were placed in the dark for 24 h before a transfer to 400 μmol photons $\cdot m^{-2} \cdot s^{-1}$ for an additional 24 h. Depending on the experiment, one, two, or three flasks were filtered independently at each sampling. Just before sampling, cell counts were performed (Coulter Multisizer II particle counter, Beckman Coulter Inc., Miami, FL, USA) and cultures tested for bacterial and fungal growth (50-μL sample in autoclaved test media: 0.5% Bactopeptone and

0.5% malt extract in filtered seawater). Cells were gently vacuum filtered onto either 0.45-μm pore size filters (Millipore, Bedford, MA, USA) or GFF filters (Whatman Inc., Newton, MA, USA). Cells were scraped from the filter and immediately frozen at –70° C or else incubated in 1 mL RNAlater (Ambion Inc., Austin, TX, USA) at 4° C overnight and transferred to –20° C for later processing.

Cells in RNAlater were thawed, amended with 100 μL sterile PBS (0.8% NaCl, 0.02% KCl, 0.144% Na_2HPO_4, 0.024% KH_2PO_4, pH 7.4), and centrifuged at 10,000*g* for 5 min. RNA was extracted from all cell pellets using the RNeasy Plant Mini Kit (Qiagen) and incubated with 6 units of DNase (Ambion) for 2 h at 37° C. These samples were then purified following the manufacturer's instructions for the RNA cleanup protocol (RNeasy Plant Mini Kit, Qiagen) or phenol/chloroform extracted and ethanol precipitated. The absence of DNA contamination in the RNA samples was tested using *GDCT*-specific primers GDCF and GDCR in a PCR. The sequence of GDCF is ATGGGTCAGATTCGTTGG and GDCR is GTGCTCCTAACCCAGTGG. The PCR profile was 94° C for 2 min followed by 30 cycles of 94° C for 10 s, 56° C for 30 s, 72° C for 1 min. The PCR amplification was performed in a 10-μL reaction containing a minimum of 100 ng of total RNA, 2.5 mM $MgCl_2$, 0.4 mM dNTPs, 4 pmol of each primer, and 0.38 units *Taq* polymerase (Promega, Madison, WI, USA). The DNA-free total RNA was quantified and assessed for quality using a GeneQuant RNA/DNA Calculator spectrophotometer (Biochrom Ltd., Cambridge, UK). Only samples with an absorbance ratio (A_{260}/A_{280}) > 1.7 were used for RT-PCR. DNA-free RNA was stored at –70° C for later analysis.

Competitive RT-PCR. Similar to the methods of Jacobs et al. (1999), a deletion competitor to the *GDCT* fragment was created by PCR using GDCR and a hybrid primer. The first 18 bp on the 5′ end of the hybrid primer were identical to GDCF. The remaining 18 bp were identical to a region 48 bp downstream from the GDCF annealing site. The sequence of the hybrid primer is ATGGGTCAGATTCGTTGGATTG-CATCTCTTCCCGCC. The PCR amplification to generate the competitor was performed in a 10-μL reaction containing 2.5 pg of a *GDCT* cDNA fragment in pCR2.1-TOPO vector, 2.5 mM $MgCl_2$, 0.4 mM dNTPs, 4 pmol of GDCR and the hybrid primer, and 0.38 units *Taq* polymerase (Promega). The PCR profile was 94° C for 2 min followed by 30 cycles of 94° C for 10 s, 56° C for 30 s, 72° C for 1 min. The PCR amplification of *GDCT* cDNA with the hybrid primer and GDCR generated a fragment 48 bp smaller than the fragment amplified by GDCF and GDCR. The deletion competitor was cloned using the TOPO TA Cloning Kit (Invitrogen) and the plasmid isolated from positive clones using the Qiaprep Spin Miniprep Kit (Qiagen). Five units of *Bam*HI were used to linearize 350 ng of plasmid DNA from positive clones. The restriction enzyme was removed with a phenol/chloroform extraction and ethanol precipitation. Competitor was transcribed *in vitro* using the MAXIscript In Vitro Transcription Kit (Ambion) with T7 RNA polymerase. As above, RNA was tested for DNA contamination and contaminated samples were treated with DNase.

The PCR primers and a deletion competitor were also constructed for amplification of the gene for carbonic anhydrase from *T. weissflogii* cDNA (*twca1*, Roberts et al. 1997). The primers for *twca1* amplification are CAF2, GGAACCGAACAC-TACTCTGTC, and CAR1, CCCATTCCCATTTCTTCATCG. The deletion in the *twca1* competitor was 55 bp. The sequence for the hybrid CA primer is GGAACCGAACACTACTCT-GTCGCCGTACCCTTGCCGAGG.

Ten to 1000 pg of both *GDCT* and *twca1* competitor RNA were combined with 200 or 400 ng of total RNA from each sample and reverse transcribed using the 1st Strand cDNA Synthesis Kit (Clontech). The resulting first-strand cDNAs were diluted 4-fold with sterile water, and 1–3 μL was used in a 10-μL PCR containing 2.5 mM $MgCl_2$, 0.4 mM dNTPs, 4 pmol of either GDCF and GDCR or CAF2 and CAR1, and 0.38 units *Taq* polymerase (Promega). The *GDCT* cDNA and its competitor cDNA were amplified using primers GDCF and GDCR with an initial denaturation step of 94° C for 2 min followed by 30 cycles of 94° C for 10 s, 56° C for 30 s, 72° C for 1 min. The *twca1* cDNA and its competitor were amplified using primers CAF2 and CAR1 with an initial denaturation step of 94° C for 2 min followed by 28 cycles of 94° C for 10 s, 58° C for 30 s, 72° C for 1 min. A minimum of three PCRs were run for each sample for both *GDCT* and *twca1* quantification. The DNA bands were separated on a 2% agarose gel, stained with SYBR Green (Molecular Probes, Eugene, OR, USA), and visualized using a FluorImager 575 (Molecular Dynamics, Amersham Biosciences Corp.) or FMBIO II Multi-View fluorescence imager (Hitachi Kokusai Electric, Tokyo, Japan). Gel images were quantified using the software ImageQuaNT v. 4.1b (Molecular Dynamics). Significant differences were determined using the software SPSS for Windows (v. 8.0.0) (SPSS Inc., Chicago, IL, USA) running a one-way analysis of variance (ANOVA) and Tukey's honestly significant difference tests.

Glycolate measurements. Experiments were conducted with cultures in early to mid-exponential growth to eliminate any effects of nutrient limitation on glycolate excretion. At each sampling, 10–30 mL of culture was syringe filtered through autoclaved 0.2 μm GTTP filters (Millipore) using autoclaved Swinnex filter holders (Millipore) and sterile rubber-free syringes. The filtrate was immediately processed or kept at 4° C for processing within a few hours. Glycolate concentrations were measured by HPLC using a modification of the 2-nitrophenylhydrazide method of Albert and Martens (1997). Samples were derivatized with 2-nitrophenylhydrazide for 1.5 h at room temperature and loaded onto a 1.5-cm concentrating column (C-18, Beckman Coulter Inc.) within the injection loop of a Gilson (model 231) autosampler (Gilsan Inc., Middleton, WI, USA). After washing the concentrator column with water, the sample was injected onto a 25-cm Beckman Ultrasphere C18 column (Beckman Coulter Inc.), and glycolate was separated from other organic acids using the ion-pairing solvent system of Albert and Martens (1997). An HPLC system with an SPD-10Avvp uv-vis detector set to 400 nm was used for sample detection (Shimadzu, Columbia, MD, USA). Glycolate concentrations were calibrated against standards of glycolate in f/2 culture media. To determine the relationship between acclimation light intensity and glycolate release, an ANOVA of regression statistics for glycolate release versus light level was performed. Significant differences between time course samples were determined using the software SPSS for Windows (v. 8.0.0) running a one-way ANOVA and Tukey's honestly significant difference tests.

RESULTS

Isolation of a. Thalassiosira weissflogii *cDNA encoding the T-protein subunit of GDC*. The predicted amino acid sequence of a partial cDNA from a sexual reproduction subtraction library (Armbrust 1999) displayed 58% identity and 65% homology to the glycine decarboxylase T-protein (GDCT) from the C4 plant *Flaveria trinervia*. RACE PCR was used to generate a full-length cDNA for this gene. The initiator methionine was assumed to be the first ATG in the full-length cDNA resulting in an open reading frame of 1245 bp and a 3′ untranslated region of 89 bp. The predicted amino acid sequence displayed homology to GDCT from both autotrophs and heterotrophs,

with the best matches found among the land plants (Fig. 1). The closest match was with the iceplant *Mesembryanthemum crystallinum* (50% identity and 64% homology).

Light dependence of GDCT *transcript abundance.* To establish whether accumulation of *T. weissflogii GDCT* mRNA is light dependent, cells acclimated to 150 μmol photons $\cdot m^{-2} \cdot s^{-1}$ of continuous light were transferred to the dark for 90 h and *GDCT* mRNA per cell was measured over time (Fig. 2). The amount of *GDCT* mRNA per cell decreased during the first 24 h of darkness despite the fact that cell division had essentially stopped after about 14 h in the dark. The continued decline in *GDCT* mRNA per cell indicates that the message was either unstable or else actively degraded. After about 2 days in the dark, a low level of *GDCT* mRNA persisted in the cells for the duration of the experiment.

Data were also normalized to total RNA to evaluate the relative changes in *GDCT* mRNA and total RNA and to ensure that variability in RNA extraction efficiency did not markedly change the observed results. Because total RNA per cell varies under changing light conditions, the absolute quantifications normalized to total RNA versus cell number were not identical. However, in every case the general trends observed for *GDCT* transcript abundance, whether normalized to cell number or total RNA, were the same (data not shown). For example, when the above data were normalized to total RNA, a decrease in *GDCT* mRNA was still observed during the dark period. This may indicate that *GDCT* mRNA abundance decreased faster than rRNA, because most total RNA is rRNA.

Thalassiosira weissflogii cultures were also acclimated to four different intensities of continuous light, and *GDCT* mRNA per cell was determined (Fig. 3). We found no significant difference between the growth rates of cells at 150 and 400 μmol photons $\cdot m^{-2} \cdot s^{-1}$ ($P = 0.998$). The growth rates at 15 and 50 μmol photons $\cdot m^{-2} \cdot s^{-1}$ were significantly lower than cells grown at either 150 or 400 μmol photons $\cdot m^{-2} \cdot s^{-1}$ ($P < 0.001$; Fig. 3). Except for one flask, cells grown at subsaturating irradiances had significantly lower *GDCT* mRNA per cell than cells maintained at growth-saturating irradiances ($P \leq 0.001$ for each pair-wise comparison; Fig. 3). There was significantly more *GDCT* mRNA in cells acclimated to 400 μmol photons $\cdot m^{-2} \cdot s^{-1}$ than to 150 μmol photons $\cdot m^{-2} \cdot s^{-1}$ ($P < 0.001$) despite the indistinguishable growth rates of these two cultures.

Transcript abundance of GDCT *over a light:dark cycle.* We also examined how steady-state levels of *GDCT* transcripts varied over a 12:12-h light:dark cycle at 100 μmol photons $\cdot m^{-2} \cdot s^{-1}$. There was no significant decrease of *GDCT* mRNA per cell after 12 h of darkness in this experiment. But within 2 h of light exposure, *GDCT* mRNA per cell increased significantly (Fig. 4). A peak in *GDCT* transcript abundance occurred at 4 h post-illumination. There was a significant decrease in *GDCT* mRNA from its peak by the end of the 12-h light period ($P < 0.001$ for all pair-wise comparisons).

GDCT *transcript abundance in a changing light environment.* To investigate the effect of changes in light conditions on *GDCT* transcript abundance, cells were acclimated to the same four continuous light intensities as described previously (Fig. 3) and then placed in the dark for 24 h before transfer to 400 μmol photons $\cdot m^{-2} \cdot s^{-1}$ of continuous light (Fig. 5, A–D). Based on the results from the dark incubation experiment (Fig. 2), a 24-h dark period was chosen to minimize transcript abundance before the increase in light intensity to ensure detection of any changes in mRNA abundance. As before, *GDCT* mRNA per cell decreased during the extended dark period. Cells began increasing *GDCT* transcript levels within 2 h of transfer to 400 μmol photons $\cdot m^{-2} \cdot s^{-1}$, regardless of the light intensity to which the cells were initially acclimated. In each case, a peak in transcript abundance was reached between 6 and 8 h after the transfer to 400 μmol photons $\cdot m^{-2} \cdot s^{-1}$. Cells acclimated to subsaturating irradiances for growth (15 and 50 μmol photons $\cdot m^{-2} \cdot s^{-1}$) had significantly higher peaks in *GDCT* transcript levels after transfer to 400 μmol photons $\cdot m^{-2} \cdot s^{-1}$ than cells acclimated to growth-saturating irradiances (150 and 400 μmol photons $\cdot m^{-2} \cdot s^{-1}$; $P < 0.001$ for all pair-wise comparisons). There was no significant difference in the peak amount of *GDCT* mRNA between cells previously acclimated to 150 μmol photons $\cdot m^{-2} \cdot s^{-1}$ and cells previously acclimated to 400 μmol photons $\cdot m^{-2} \cdot s^{-1}$. The peak in *GDCT* transcripts for cells acclimated to 50 μmol photons $\cdot m^{-2} \cdot s^{-1}$ was significantly lower than the peak observed for cells acclimated to 15 μmol photons $\cdot m^{-2} \cdot s^{-1}$ ($P < 0.01$). Twenty-four hours after a shift to 400 μmol photons $\cdot m^{-2} \cdot s^{-1}$, there was no significant difference in the amount of *GDCT* mRNA per cell in cultures acclimated to 50, 150, or 400 μmol photons $\cdot m^{-2} \cdot s^{-1}$. In contrast, cells acclimated to 15 μmol photons $\cdot m^{-2} \cdot s^{-1}$ maintained a 10-fold greater amount of *GDCT* mRNA per cell throughout the light period. For cells acclimated to this lowest irradiance before the light shift, the amount of *GDCT* mRNA per cell remained significantly higher than any of the other experiments both at 12 and 24 h ($P < 0.001$ for all pair-wise comparisons).

Transcript abundance of twca1 in a changing light environment. Transcript levels for *twca1*, which encodes carbonic anhydrase, were monitored to determine whether transcripts of a gene from a closely related pathway (the carbon-concentrating mechanism [CCM]) displayed a similar response to changes in light intensity. During the dark period, there was a slight decrease in *twca1* mRNA per cell ($P < 0.05$; Fig. 5E). However, unlike *GDCT* mRNA, *twca1* mRNA per cell dropped even lower after 2 h in the light and remained low for 6 h before climbing to a peak by the end of the experiment. A similar pattern in *twca1* transcripts was observed for each of the four light transition experiments (data not shown).

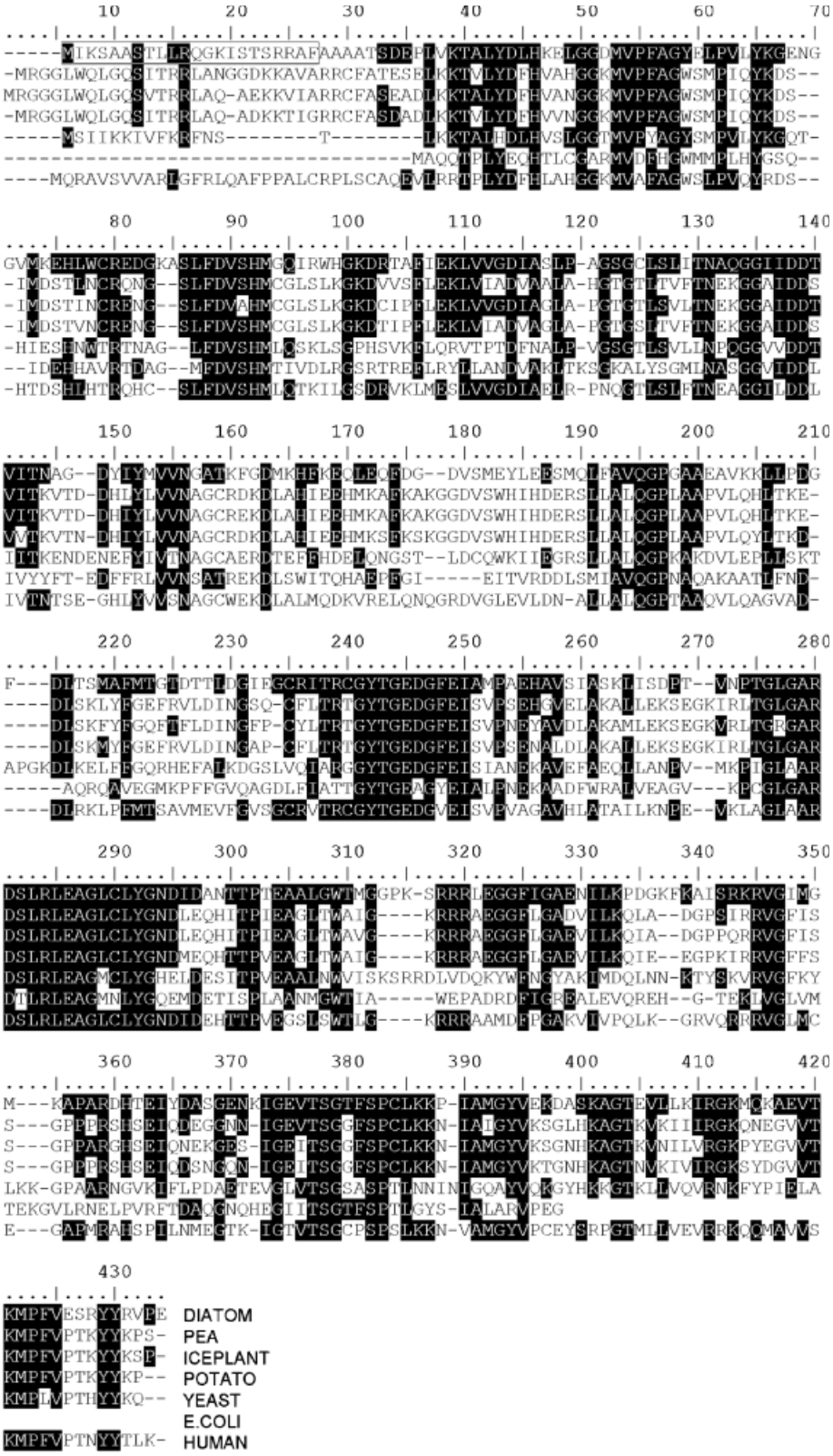

FIG. 1. Inferred amino acid sequence of the cDNA *GDCT* from *Thalassiosira weissflogii* (labeled as diatom) aligned with the amino acid sequences of pea (*Pisum sativum*), GenBank accession P49364; iceplant (*Mesembryanthemum crystallinum*), GenBank accession P93256; potato (*Solanum tuberosum*), GenBank accession P54260; yeast (*Saccharomyces cerevisiae*), GenBank accession NP_010302; *Escherichia coli* K12, GenBank accession NP_417381; and human (*Homo sapiens*), GenBank accession P48728. Black boxes highlight identities with the *T. weissflogii* sequence. Dashes represent gaps inserted for maximum alignment. The predicted mitochondrial presequence for *T. weissflogii* is boxed. Numbers indicate amino acid sequence length.

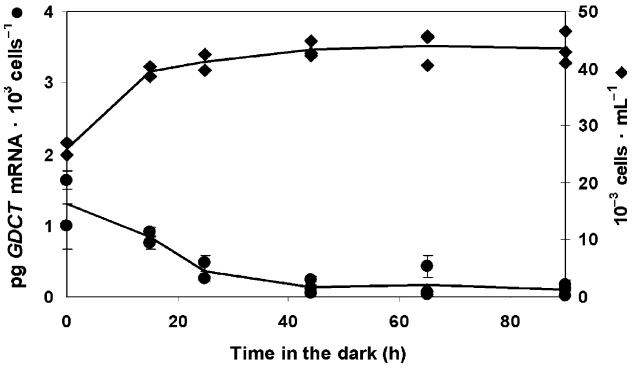

FIG. 2. Time course of *GDCT* mRNA concentration (circles) and cell concentration (diamonds) for *Thalassiosira weissflogii* cultures acclimated to 150 μmol photons · m^{-2} · s^{-1} before being placed in the dark for 90 h. Each symbol represents an independent flask. Error bars are SDs from three or more PCRs from the same flask. Lines are drawn through the mean at each time point.

Glycolate excretion. To determine the effect of different light intensities on glycolate excretion, HPLC was used to measure concentrations of glycolate in the media of cells acclimated to 15, 50, 100, and 400 μmol photons · m^{-2} · s^{-1}. No significant correlation between glycolate released into the media and light level was detected ($r^2 = 0.19$, $P = 0.24$, data not shown). Also, no significant change in glycolate release per cell over time was detected when cells were maintained at two of these light intensities, 15 and 100 μmol photons · m^{-2} · s^{-1}, over a 48-h period (Fig. 6A). Furthermore, a period of darkness also did not change the amount of glycolate released from cells acclimated to 100 μmol photons · m^{-2} · s^{-1}, placed in the dark for 24 h and returned to 100 μmol photons · m^{-2} · s^{-1} (Fig. 6A). In contrast, cells acclimated to either 15 or 50 μmol photons · m^{-2} · s^{-1}, transferred to 24 h of darkness, and subsequently introduced to 400 μmol photons · m^{-2} · s^{-1} released a significant amount of glycolate into the media within 6 and 8 h, respectively ($P < 0.001$; Fig. 6B). The peak in glycolate release from the culture acclimated to 15 μmol photons · m^{-2} · s^{-1} was significantly greater than the peak release from the culture acclimated to 50 μmol photons · m^{-2} · s^{-1} ($P < 0.001$; Fig. 6B). Importantly, the culture acclimated to 15 μmol photons · m^{-2} · s^{-1} and transferred to 400 μmol photons · m^{-2} · s^{-1} (Fig. 6B) released two to three times more glycolate than the culture maintained in constant light of 15 μmol photons · m^{-2} · s^{-1} (Fig. 6A).

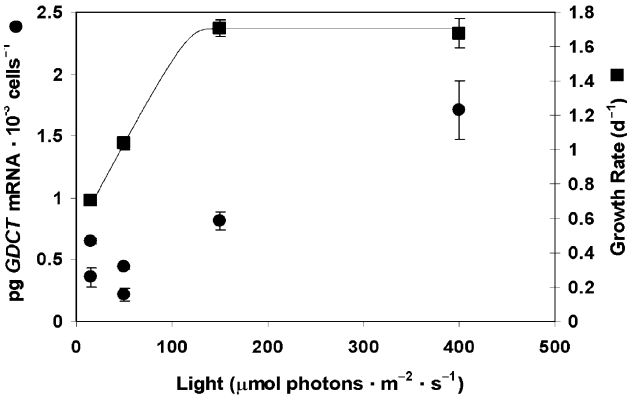

FIG. 3. *GDCT* mRNA concentrations (circles) and growth rates (squares) for *Thalassiosira weissflogii* cultures acclimated to four different light intensities: 15, 50, 150, and 400 μmol photons · m^{-2} · s^{-1}. Each symbol represents data from an independent flask. Error bars represent SDs of three or more PCRs from the same flask (circles) or three successive transfers after acclimation (squares).

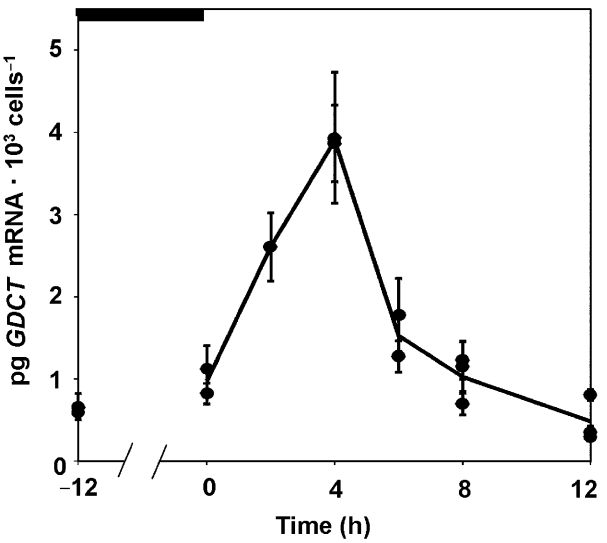

FIG. 4. *GDCT* mRNA concentrations in *Thalassiosira weissflogii* cells acclimated to a 12:12-h light:dark cycle at 100 μmol photons · m^{-2} · s^{-1}. Each circle represents an independent flask. Error bars indicate SDs from three or more PCRs from the same flask. Black bar indicates dark interval. The line is drawn through the mean at each time point.

DISCUSSION

We identified a cDNA in *T. weissflogii* with an inferred amino acid sequence homologous to the T-protein of GDC, a central enzyme of the photorespiratory pathway in autotrophs. In eukaryotes, GDC is localized to the mitochondria (Motokawa and Kikuchi 1971, Oliver 1994). The *T. weissflogii* GDCT contained a putative mitochondrial transit peptide rich in positively charged and nonpolar residues, a fundamental characteristic of mitochondrial presequences in plants (Chaumont and Boutry 1995) that has also been observed in diatoms (Liaud et al. 2000). In addition, the splice site matched the consensus for mitochondrial targeting peptides in plants: R X F ↓ S/A, where ↓ represents the splice site and X indicates any amino acid (Chaumont and Boutry 1995). Our results strongly suggest that the *GDCT* sequence from *T. weissflogii* codes for the T-protein of the GDC complex and that accumulation of transcripts for this gene is

light dependent, consistent with a role of this enzyme in photorespiration. We have demonstrated a correlation between light intensity and steady-state levels of *GDCT* mRNA in *T. weissflogii* cells. In addition, *T. weissflogii* cells rapidly accumulate *GDCT* transcripts (within 2 h) upon transfer of cells from the dark to the light. In land plants, the response of GDC gene transcription to changes in light intensity also occurs on the order of hours (Srinivasan et al. 1993, Vauclare et al. 1998). Under the most extreme light shifts in our experiments, we observed the release of the photorespiratory compound glycolate concurrent with an increase in *GDCT* transcript abundance, providing further evidence of a correlation between *GDCT* mRNA levels and photorespiration.

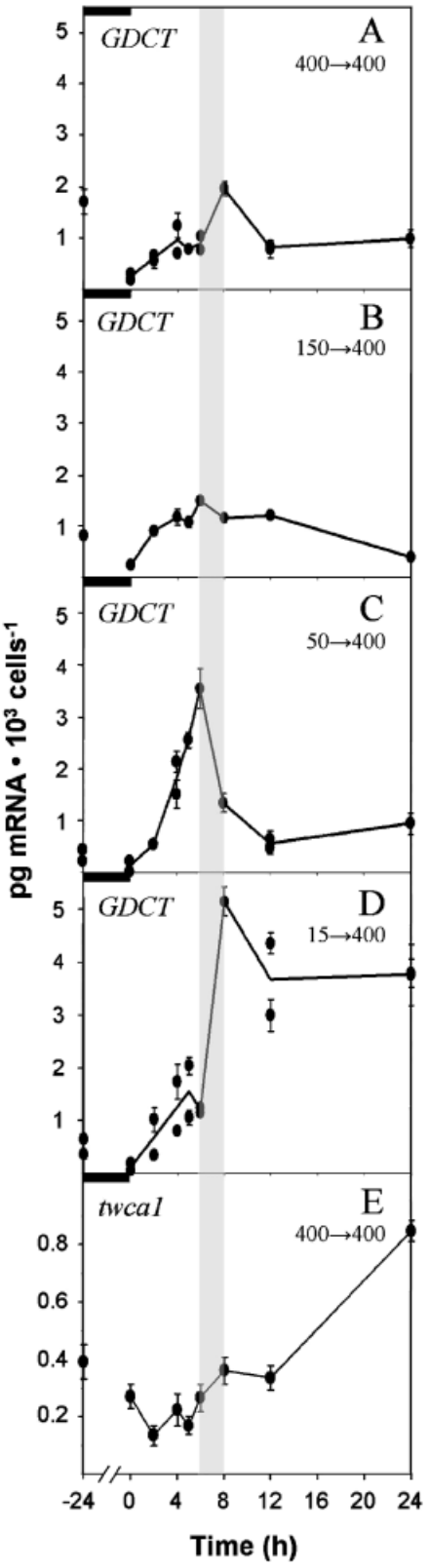

Our experiments also demonstrate that *GDCT* transcript abundance may be a more sensitive marker for photorespiration than the more commonly measured release of glycolate (Fogg 1983). Based on our results, most of the glycolate produced by photorespiration appears to be recycled within the cell. Cells acclimated to constant light intensities did not release more glycolate at higher irradiances. Yet *GDCT* transcript abundance correlated well with constant light intensity: highest amounts of *GDCT* mRNA were observed at the light intensity well above growth saturation. This suggests that the cells had up-regulated the photorespiratory pathway and were recycling much of the glycolate produced by oxygen fixation. Importantly, even though glycolate was not released from the cell, photorespiration would still have facilitated the conversion of fixed carbon and nitrogen to CO_2 and NH_3. The marker we chose (*GDCT*) encodes a subunit of the enzyme that catalyzes the reaction producing both CO_2 and NH_3.

An increase in glycolate release was observed only when *T. weissflogii* cells were first acclimated to a low light intensity and then transferred to the highest light intensity. The most "light shocked" of these cultures (cells acclimated to 15 μmol photons $\cdot m^{-2} \cdot s^{-1}$ before transfer to 400 μmol photons $\cdot m^{-2} \cdot s^{-1}$) also had a peak in *GDCT* transcripts nearly three times that of the high-light acclimated cultures, and the levels of *GDCT* mRNA did not return to steady state by the end of the 24 h in high light as was seen with all the other cultures. This suggests that not only did the experimental conditions induce photorespiration, but the production of glycolate due to oxygen fixation exceeded the ability of the cell to further metabolize it.

Glycolate production in excess of metabolism may indicate a rate-limiting step in the photorespiratory pathway that prevents the rapid recycling of glycolate, resulting in release of this compound from the cell. Stewart and Codd (1981) found evidence for end-product inhibition of glycolate dehydrogenase, the

FIG. 5. Concentration of *GDCT* mRNA (A–D) or *twca1* mRNA (E) in *Thalassiosira weissflogii* cells acclimated to (A) 400, (B) 150, (C) 50, (D) 15, and (E) 400 μmol photons $\cdot m^{-2} \cdot s^{-1}$ before transfer to the dark (–24 h). At t = 0 h, all cultures were transferred to a light intensity of 400 μmol photons $\cdot m^{-2} \cdot s^{-1}$. Each circle represents an independent flask. Error bars are SDs from three or more PCRs from the same flask. Black bars indicate dark interval. Peaks are highlighted by gray area. Lines are drawn through the mean at each time point. Note change in *y*-axis scale for E.

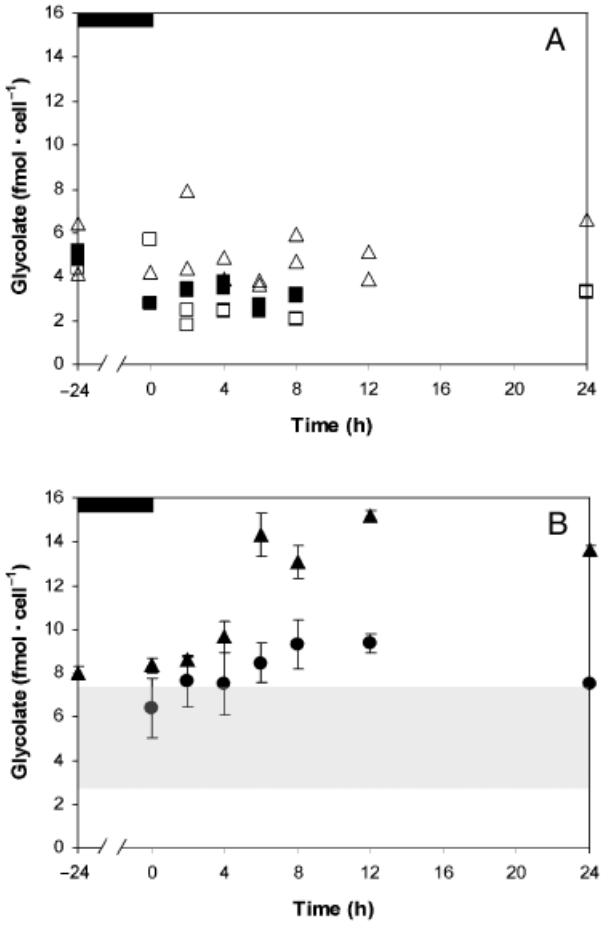

FIG. 6. Extracellular concentrations of glycolate in the culture media. (A) Cells were maintained in continuous light of 15 μmol photons $\cdot m^{-2} \cdot s^{-1}$ (open triangles) and 100 μmol photons $\cdot m^{-2} \cdot s^{-1}$ (open squares) or acclimated to 100 μmol photons $\cdot m^{-2} \cdot s^{-1}$, transferred to the dark for 24 h, and reintroduced to 100 μmol photons $\cdot m^{-2} \cdot s^{-1}$ (closed squares). (B) Cells were acclimated to 15 μmol photons $\cdot m^{-2} \cdot s^{-1}$ (closed triangles) or 50 μmol photons $\cdot m^{-2} \cdot s^{-1}$ (closed circles) of continuous light, transferred to the dark for 24 h, and introduced to 400 μmol photons $\cdot m^{-2} \cdot s^{-1}$. Shading indicates 2 SDs from the mean of the 15 μmol photons $\cdot m^{-2} \cdot s^{-1}$ continuous light culture. Error bars are SDs for three replicate measurements from the same flask. Duplicate symbols indicate duplicate measurements from the same flask. Black bar represents the time the cultures (closed symbols) spent in the dark.

enzyme that catalyzes the oxidation of glycolate to glyoxylate in green algae. If the glycolate oxidizing enzyme in *T. weissflogii* is similarly regulated, then this may explain the release of glycolate when photorespiration is up-regulated. The rate of extracellular glycolate production in our cultures (about $1\,nmol \cdot h^{-1} \cdot 10^6$ cells^{-1}) was about an order of magnitude less than the rates determined for the chlorophyte *Dunaliella tertiolecta* (14–30 $nmol \cdot h^{-1} \cdot 10^6$ cells^{-1}; Leboulanger et al. 1998). This difference is consistent with a lower specific activity of glycolate dehydrogenase in green algae compared with glycolate oxidases found in many other autotrophs (Tolbert 1974). A low specific activity may result in more glycolate escaping the cell before oxidation to glyoxylate occurs. The maximum concentration of glycolate released into the media of our cultures (60.8 $\mu g \cdot L^{-1}$) is comparable with concentrations found in mesotrophic (74 $\mu g \cdot L^{-1}$) and oligotrophic (17 $\mu g \cdot L^{-1}$) sites of the eastern Atlantic Ocean (Leboulanger et al. 1997). The cultures used in our experiments probably had higher cell concentrations than these field samples, but they were also free of heterotrophs that could consume the released glycolate. We also note that the highest light levels achieved by our growth chamber were much lower than the incident PAR in most surface waters, suggesting that photorespiration and glycolate release may be common phenomena.

For cells that are mixed into a high light environment, the protection from photooxidative damage provided by photorespiration may outweigh the potential loss of carbon and nitrogen due to the production of glycolate, CO_2, and NH_3. Based on turbulent diffusion theory and common oceanographic conditions, Lande and Wood (1987) estimated that phytoplankton cells will cycle every few days between the light-limiting conditions of a deep thermocline and the often photoinhibiting conditions of surface waters. Sudden shifts in light intensity coupled with light levels above saturation for the photosynthetic apparatus may result in the production of a high-energy state "triplet" chlorophyll, which in the presence of oxygen can form highly reactive oxygen radicals (Buchanan et al. 2000). Photosynthetic cells have developed a number of mechanisms for dealing with the input of excess light energy in the presence of oxygen. These include energy dissipation via fluorescence or production of heat (Powles 1984), the xanthophyll cycle (Baroli and Niyogi 2000), cyclic electron flow (Shikanai et al. 2002), chlororespiration (Nixon 2000, Dijkman and Kroon 2002), and the Mehler reaction (Powles 1984). As an energy-demanding and oxygen-consuming pathway, photorespiration has also been shown in numerous studies to have a photoprotective role (Wingler et al. 2000). Using mutants of tobacco (*Nicotiana tabacum* L.) defective in enzymes of the photorespiratory pathway, a direct relationship has been found between the inability of plants to photorespire under high light conditions and enhanced photoinhibition in the form of chl degradation (Kozaki and Takeba 1996, Yamaguchi and Nishimura 2000). In addition, studies monitoring electron flow found that photorespiration is essential for protection of the photosynthetic apparatus in high light (Wu et al. 1991, Park et al. 1996, Igamberdiev et al. 2001).

When light is limiting, however, the effects of photorespiration may not be beneficial to the cell. Under conditions of elevated O_2 relative to CO_2, photorespiration can be detrimental to cells by inhibiting carbon fixation. To help increase CO_2 concentrations in the cell, many algae have developed a carbon-concentrating mechanism (CCM). One of the key enzymes of the CCM, carbonic anhydrase, catalyzes

the reversible conversion of bicarbonate to CO_2. In our experiments, we measured the abundance of transcripts for the gene *twca1* hypothesized to code for carbonic anhydrase in *T. weissflogii*. Although there is no direct evidence that TWCA1 is involved in the CCM of *T. weissflogii*, Lane and Morel (2000) demonstrated correlations between *twca1* transcript abundance, TWCA1 protein levels, and carbonic anhydrase activity in *T. weissflogii* cells switched from high to low CO_2 concentrations. Unlike *GDCT*, genes that encode carbonic anhydrases in microalgae appear to be regulated by the inorganic carbon concentration of the medium, not by light or O_2 concentration (Sultemeyer 1998). In our experiments, we did not find an appreciable increase in *twca1* until 12 h after a shift from darkness to light. Likely, the concentration of CO_2 in the cell was initially sufficient to sustain photosynthesis for the first several hours, perhaps accounting for the delay in *twca1* mRNA increase. These results support the idea that accumulation of *GDCT* transcripts is regulated by a different mechanism from *twca1* transcripts.

Nevertheless, dynamic interactions likely exist between photosynthetic carbon fixation, photorespiration, and the CCM. All three are dependent to some extent on the constantly fluctuating concentrations of intracellular O_2 and dissolved inorganic carbon, which in turn are dependent to some extent on the availability of light. For example, our results show that cells acclimated to a 12:12-h light:dark cycle have a peak in *GDCT* transcripts early in the light period with a decrease in *GDCT* transcripts before the dark period. This pattern is reminiscent of a diel periodicity. The transcription of the gene for the large subunit of RUBISCO in cyanobacteria and a prymnesiophyte were also found to follow a diel periodicity, though the phase was slightly offset from daylight with transcription increasing before dawn in anticipation of the light (Wyman 1999, Paul et al. 2000). Furthermore, Paul et al. (2000) demonstrated a similar diel pattern in both the activity of RUBISCO and carbon fixation in each of these organisms. Whether the fluctuations in *GDCT* transcripts can be attributed to a circadian rhythm or are somehow linked to a periodicity in RUBISCO abundance remains speculative. It is possible that the pathways for both carbon and oxygen fixation (photosynthesis and photorespiration) are tightly coupled to daylight to optimize production of enzymes during the day and down-regulate enzyme production in anticipation of the night.

In algal cells, photorespiration not only decreases photosynthetic assimilation when the active sites of RUBISCO are occupied by O_2 and fixed carbon is released as CO_2, but may additionally cause the release of organic carbon in the form of glycolate. Using a molecular marker for an enzyme of the photorespiratory pathway (*GDCT*) and measurements of a photorespiratory byproduct (glycolate), we have begun to uncover the dynamics of photorespiratory metabolism in the centric diatom *T. weissflogii*. Our results suggest that even cells acclimated to constant light intensities appear to be photorespiring. However, cells do not appear to release a substantial amount of their fixed carbon as glycolate until the production of glycolate overwhelms the ability of the cell to recycle it in the photorespiratory pathway. This implies that cells in stratified environments may release less of their fixed carbon as glycolate than cells mixed between light-limiting depths and photoinhibiting surface waters. Under these conditions, glycolate may contribute significantly to labile DOC in the upper ocean. In the dilute marine environment, labile DOC is essential for microbial production. With the development of *GDCT* into a more universal algal probe, coupled with measurements of glycolate, we are beginning to assess the occurrence and prevalence of photorespiration in the marine environment and investigate photorespiration as a mechanism for DOC entry into the marine food web.

We thank Rose Ann Cattolico and Mary Jane Perry for their many helpful discussions and insights. We also thank Tatiana Rynearson, Winnie Lau, and Heather Galindo for their comments and reviews of this work. Finally, we are indebted to Meredith Vaughan for her tireless help in the laboratory. This research was funded by the Biotechnological Investigations-Ocean Margins Program, Biological and Environmental Research (BER), U.S. Department of Energy (grant no. DE-FG03-00ER62982).

Albert, D. B. & Martens, C. S. 1997. Determination of low-molecular-weight organic acid concentrations in seawater and pore-water samples via HPLC. *Mar. Chem.* 56:27–37.

Al-Hasan, R. H. & Coughlan, S. J. 1976. A method for the determination of glycolic acid in the extracellular products of cultured and natural phytoplankton populations. *J. Exp. Mar. Biol. Ecol.* 25:141–9.

Armbrust, E. V. 1999. Identification of a new gene family expressed during the onset of sexual reproduction in the centric diatom *Thalassiosira weissflogii*. *Appl. Environ. Microbiol.* 65:3121–8.

Armbrust, E. V., Olson, R. J. & Chisholm, S. W. 1990. Role of light and the cell cycle on the induction of spermatogenesis in a centric diatom. *J. Phycol.* 26:470–8.

Baines, S. B. & Pace, M. L. 1991. The production of dissolved organic matter by phytoplankton and its importance to bacteria: patterns across marine and freshwater systems. *Limnol. Oceanogr.* 36:1078–90.

Baroli, I. & Niyogi, K. K. 2000. Molecular genetics of xanthophyll-dependent photoprotection in green algae and plants. *Phil. Trans. R. Soc. Lond. B* 355:1385–94.

Beardall, J. 1989. Photosynthesis and photorespiration in marine phytoplankton. *Aquat. Bot.* 34:105–30.

Brand, L. E., Guillard, R. R. L. & Murphy, L. S. 1981. A method for the rapid and precise determination of acclimated phytoplankton reproduction rates. *J. Plankton Res.* 3:193–201.

Buchanan, B. B., Gruissem, W. & Jones, R. L. [Eds.] 2000. *Biochemistry and Molecular Biology of Plants*. American Society of Plant Physiologists, Rockville, MD, 1367 pp.

Buck, K. R. & Newton, J. 1995. Fecal pellet flux in Dabob Bay during a diatom bloom: contribution of microzooplankton. *Limnol. Oceanogr.* 40:306–15.

Burris, J. E. 1977. Photosynthesis, photorespiration, and dark respiration in eight species of algae. *Mar. Biol.* 39:371–9.

Chaumont, F. & Boutry, M. 1995. Protein import into plant mitochondria. *In* Levings, C. S. & Vasil, I. K. [Eds.] *The Molecular Biology of Plant Mitochondria*. Kluwer Academic Publishers, Dordrecht, The Netherlands, pp. 207–235.

Chrost, R. H. & Faust, M. A. 1983. Organic carbon release by phytoplankton: its composition and utilization by bacterioplankton. *J. Plankton Res.* 5:477–93.

Dijkman, N. A. & Kroon, B. M. A. 2002. Indications for chlororespiration in relation to light regime in the marine diatom *Thalassiosira weissflogii*. *J. Photochem. Photobiol. B* 66:179–87.

Duxbury, A. C., Duxbury, A. B. & Sverdrup, K. A. 2000. *An Introduction to the World's Oceans*. 6th ed. McGraw Hill, Boston, 528 pp.

Fogg, G. E. 1983. The ecological significance of extracellular products of phytoplankton photosynthesis. *Bot. Mar.* 26:3–14.

Guillard, R. R. L. 1975. Culture of phytoplankton for feeding marine invertebrates. *In* Smith, W. L. & Chaney, M. H. [Eds.] *Culture of Marine Invertebrate Animals*. Plenum Press, New York, pp. 29–60.

Hall, T. A. 1999. BioEdit: a user-friendly biological sequence alignment editor and analysis program for Windows 95/98/NT. *Nucl. Acids Symp. Ser.* 41:95–8.

Hellebust, J. A. 1965. Excretion of some organic compounds by marine phytoplankton. *Limnol. Oceanogr.* 10:192–206.

Igamberdiev, A. U., Bykova, N. V., Lea, P. J. & Gardenstrom, P. 2001. The role of photorespiration in redox and energy balance of photosynthetic plant cells: a study with a barley mutant deficient in glycine decarboxylase. *Physiol. Plantar.* 111:427–38.

Jacobs, M. A., Connell, L. & Cattolico, R. A. 1999. A conserved His-Asp signal response regulator-like gene in *Heterosigma akashiwo* chloroplasts. *Plant Mol. Biol.* 41:645–55.

Keys, A. J., Bird, I. F., Cornelius, M. J., Lea, P. J., Wallsgrove, R. M. & Miflin, B. J. 1978. Photorespiratory nitrogen cycle. *Nature* 275:741–3.

Kikuchi, G. & Hiraga, K. 1982. The mitochondrial glycine cleavage system: unique features of the glycine decarboxylation. *Mol. Cell Biochem.* 45:137–49.

Kozaki, A. & Takeba, G. 1996. Photorespiration protects C3 plants from photooxidation. *Nature* 384:557–60.

Lande, R. & Wood, A. M. 1987. Suspension times of particles in the upper ocean. *Deep-Sea Res.* 34:61–72.

Lane, T. W. & Morel, F. M. M. 2000. Regulation of carbonic anhydrase expression by zinc, cobalt, and carbon dioxide in the marine diatom *Thalassiosira weissflogii*. *Plant Physiol.* 123:345–52.

Leboulanger, C., Martin-Jezequel, V., Descolas-Gros, C., Sciandra, A. & Jupin, H. J. 1998. Photorespiration in continuous cultures of *Dunaliella tertiolecta* (Chlorophyta): relationships between serine, glycine, and extracellular glycolate. *J. Phycol.* 34:651–4.

Leboulanger, C., Oriol, L., Jupin, H. & Descolas-Gros, C. 1997. Diel variability of glycolate in the eastern tropical Atlantic Ocean. *Deep-Sea Res.* 44:2131–9.

Liaud, M.-F., Lichtle, C., Apt, K., Martin, W. & Cerff, R. 2000. Compartment-specific isoforms of TP1 and GAPDH are imported into diatom mitochondria as a fusion protein: evidence in favor of a mitochondrial origin of the eukaryotic glycolytic pathway. *Mol. Biol. Evol.* 17:213–23.

Longhurst, A. R. & Harrison, W. G. 1989. The biological pump: profiles of plankton production and consumption in the upper ocean. *Progr. Oceanogr.* 22:47–123.

Malinsky-Rushansky, N. Z. & Legrand, C. 1996. Excretion of dissolved organic carbon by phytoplankton of different sizes and subsequent bacterial uptake. *Mar. Ecol. Prog. Ser.* 132: 249–55.

Motokawa, Y. & Kikuchi, G. 1971. Glycine metabolism in rat liver mitochondria. V. Intramitochondrial localization of the reversible glycine cleavage system and serine hydroxymethyltransferase. *Arch. Biochem. Biophys.* 146:461–6.

Mouillon, J. M., Aubert, S., Bourguignon, J., Gout, E., Douce, R. & Rebeille, F. 1999. Glycine and serine catabolism in non-photosynthetic higher plant cells: their role in C1 metabolism. *Plant J.* 20:197–205.

Nagata, T. 2000. Heterotrophic bacteria and the dynamics of dissolved organic material. *In* Kirchman, D. L. [Ed.] *Microbial Ecology of the Oceans*. Wiley, New York, pp. 121–152.

Nelson, D. M., Tréguer, P., Brzezinski, M. A., Leynaert, A. & Quéguiner, B. 1995. Production and dissolution of biogenic silica in the ocean: revised global estimates, comparison with regional data and relationship to biogenic sedimentation. *Glob. Biogeochem. Cycle* 9:359–72.

Nixon, P. J. 2000. Chlororespiration. *Phil. Trans. R. Soc. Lond. B* 355:1541–7.

Oliver, D. J. 1994. The glycine decarboxylase complex from plant mitochondria. *Annu. Rev. Plant Physiol. Plant Mol. Biol.* 45:323–37.

Oliver, D. J. 1998. Photorespiration and the C_2 cycle. *In* Raghavendra, A. S. [Ed.] *Photosynthesis: A Comprehensive Treatise*. Cambridge University Press, Cambridge, pp. 173–182.

Oliver, D. J., Neuburger, M., Bourguignon, J. & Douce, R. 1990. Glycine metabolism by plant mitochondria. *Physiol. Plantar.* 80:487–91.

Pant, A. & Fogg, G. E. 1976. Uptake of glycolate by *Skeletonema costatum* (Grev.) Cleve in bacterized cultures. *J. Exp. Mar. Biol. Ecol.* 22:227–34.

Park, Y. I., Chow, W. S., Osmond, C. B. & Anderson, J. M. 1996. Electron transport to oxygen mitigates against photoinactivation of photosystem II in vivo. *Photosynth. Res* 50:23–32.

Paul, J. H., Kang, J. B. & Tabita, F. R. 2000. Diel periodicity of regulation of *rbcL* transcription in a cyanobacterium and a prymnesiophyte. *Mar. Biotechnol.* 2:429–36.

Powles, S. B. 1984. Photoinhibition of photosynthesis induced by visible light. *Annu. Rev. Plant Physiol.* 35:15–44.

Roberts, S. B., Lane, T. W. & Morel, F. M. M. 1997. Carbonic anhydrase in the marine diatom *Thalassiosira weissflogii* (Bacillariophyceae). *J. Phycol.* 33:845–50.

Scharek, R., Tupas, L. M. & Karl, D. M. 1999. Diatom fluxes to the deep sea in the oligotrophic North Pacific gyre at Station ALOHA. *Mar. Ecol. Prog. Ser.* 182:55–67.

Shikanai, T., Munekage, Y. & Kimura, K. 2002. Regulation of proton-to-electron stoichiometry in photosynthetic electron transport: physiological function in photoprotection. *J. Plant Res.* 115:3–10.

Srinivasan, R., Berndt, W. A. & Oliver, D. J. 1993. Coordinated expression of photosynthetic and photorespiratory genes. *In* Brennicke, A. & Kuech, U. [Eds.] *Plant Mitochondria: With Emphasis on RNA Editing and Cytoplasmic Male Sterility.* VCH Publishers, New York, pp. 241–50.

Stewart, R. & Codd, G. A. 1981. Glycolate and glyoxylate excretion by *Sphaerocystis schroeteri* Chlorophyceae. *Br. Phycol. J.* 16:177–82.

Sultemeyer, D. 1998. Carbonic anhydrase in eukaryotic algae: characterization, regulation, and possible function during photosynthesis. *Can. J. Bot.* 76:962–72.

Thompson, J. D., Higgins, D. G. & Gibson, T. J. 1994. CLUSTAL W: improving the sensitivity of progressive multiple sequence alignment through sequence weighting, position specific gap penalties and weight matrix choice. *Nucleic Acids Res.* 22: 4673–80.

Tolbert, N. E. 1974. Photorespiration. *In* Stewart, W. D. P. [Ed.] *Algal Physiology and Biochemistry.* University of California Press, Berkeley CA, pp. 474–504.

Turner, S. R., Hellens, R., Ireland, R., Ellis, N. & Rawsthorne, S. 1993. The organisation and expression of the genes encoding the mitochondrial glycine decarboxylase complex and serine hydroxymethyltransferase in pea (*Pisum sativum*). *Mol. Gen. Genet.* 236:402–8.

Vauclare, P., Macherel, D., Douce, R. & Bourguignon, J. 1998. The gene encoding T protein of the glycine decarboxylase complex involved in the mitochondrial step of the photorespiratory pathway in plants exhibits features of light-induced genes. *Plant Mol. Biol.* 37:309–18.

Verity, P. G. 1981. Effects of temperature, irradiance, and day length on the marine diatom *Leptocylindrus danicus* Cleve. II. Excretion. *J. Exp. Mar. Biol. Ecol.* 55:159–69.

Wingler, A., Lea, P. J., Quick, W. P. & Leegood, R. C. 2000. Photorespiration: metabolic pathways and their role in stress protection. *Phil. Trans. R. Soc. Lond. B* 355:1517–29.

Wright, R. T. & Shah, N. M. 1975. The trophic role of glycolic acid in coastal seawater. I. Heterotrophic metabolism in seawater and bacterial cultures. *Mar. Biol.* 33:175–83.

Wu, J., Neimanis, S. & Heber, U. 1991. Photorespiration is more effective than the Mehler reaction in protecting the photosynthetic apparatus against photoinhibition. *Bot. Acta* 104: 283–91.

Wyman, M. 1999. Diel rhythms in ribulose-1,5-bisphosphate carboxylase/oxygenase and glutamine synthetase gene expression in a natural population of marine picoplanktonic cyanobacteria (*Synechococcus* spp.). *Appl. Environ. Microbiol.* 65:3651–9.

Yamaguchi, K. & Nishimura, M. 2000. Reduction to below threshold levels of glycolate oxidase activities in transgenic tobacco enhances photoinhibition during irradiation. *Plant Cell Physiol.* 41:1397–406.

Zar, J. H. 1996. *Biostatistical Analysis*. Prentice Hall, Englewood Cliffs, New Jersey, 718 pp.

Zlotnik, I. & Dubinsky, Z. 1989. The effect of light and temperature on DOC excretion by phytoplankton. *Limnol. Oceanogr.* 34:831–9.